What Can Be Interesting in the Analysis of Crowded Solar Bursts?

A.A. Stanislavsky[1,2], A.A. Konovalenko[1], A.A. Koval[1], V.V. Dorovsky[1], Ph. Zarka[3], H.O. Rucker[4]

[1] Institute of Radio Astronomy, National Academy of Sciences of Ukraine, Kharkiv, Ukraine;
[2] V.N. Karazin Kharkiv National University, Kharkiv, Ukraine;
[3] LESIA, Observatoire de Paris, CNRS, Meudon Cedex, 92195, France;
[4] Space Research Institute, Austrian Academy of Sciences, Graz, Austria;

E mail (a.a.stanislavsky@rian.kharkov.ua).

Abstract. At decameter wavelengths the radio astronomy observations reveal a wide variety of solar bursts. They are associated with solar activity manifestations such as movements of electron beams and shock waves in solar corona, flare-related events, coronal mass ejections and others. The analysis of burst features allows one to use them as probing signals which comprise useful information about solar corona parameters and their changes over time. By frequency-time measurements of different types of solar bursts occurred about the same time one can provide a comparative study of their properties, complementing the missing pieces in the complex mosaic of solar events. In this purpose we discuss features of their signal processing by the gradient filtration, as applied to quasi-periodic bursts like a zebra pattern related to Bernstein modes. The measured frequency periodicity of the bursts gives a chance to determine the magnetic field strength in upper corona around the protracted solar minimum of solar activity.

Keywords: Coronal magnetic field, Radio bursts, Decameter range, Zebra pattern.

Introduction

The display of solar radio data in the form of a dynamic spectrum (intensity of radio emission in frequency and time) is a conventional approach for the visualization of solar bursts. Such 2D pseudo-color images permit ones to distinguish one burst (or even a set of bursts) from others, determine their frequency drift rates and much more. Radio observations of solar activity in decameter wavelengths demonstrate a wide variety of solar bursts different in frequency, time, polarization and intensity properties (Melnik et al., 2005 and references therein). The most population of them, type III bursts, is often accompanied with chains of short, narrow-band emission (type IIIb bursts). Solar flares and solar mass ejections (CMEs) produce shock waves associated with type II bursts. In addition to these types of bursts many other radio events (strias, drift pairs, fiber bursts and so on) can be recorded simultaneously or one after the other. Therefore, sometimes it is not easy to recognize what kind of a burst was recorded in a particular case because of its strong mixing with other bursts. In this connection it should be also pointed out that the digital progress in the radio astronomy equipment steeply improves the observation resolution and sensitivity helpful to detect fine structures in solar bursts. Consequently, the analysis of solar burst records makes a challenge to understand causes why such bursts appeared together, how to separate a crowd of different solar bursts in isolated bursts, and what kind of information about coronal properties it is possible to find out of them.

In this report we propose to use the gradient analysis of dynamic spectra for this purpose. As an example, the approach was tested for the observation of a complex structure on 2 June of 2011. It shows that gradient manipulations can serve as an efficient tool for dynamic spectrum processing in radio astronomy.

Gradient Analysis Algorithm

In this section we will present the algorithm for gradient filtration of complex structures on dynamic spectra of solar radio emission. Dynamic spectrum of solar events as a pseudo-color image consists of many structural units, and an experimentalist interprets them via simplified objects (tracks) or exaggerated features often facilitating clear perception and comprehension of observed phenomena. Ones of such basic units are edges. They are recognized from gradient differences on images. Edges and their form show a hierarchy of image structures often looking like amazing ridges and valleys at different scales of spectral observations. It turns out that the gradient manipulations are very useful for the study of crowded solar bursts from their images on dynamical spectra. The flexibility of gradient domain manipulation gives the high level control in the gradient scale space suppressing ones and amplifying other scale features.

Gradient domain is an intuitive representation for image contrast, and too steep edges (like a Heaviside step function) create remarkable derivative discontinuities associated with image brightness (Fattal et al., 2002). Another source of gradient discontinuities is a noise present in all dynamic spectra. Solar bursts are always noise-like signals. Therefore, it is impossible

to avoid a smoothing of such an image. In this case the very convenient way is to convolve the original spectrum $I(x, y)$ with a Gaussian kernel G, namely

$$I * G = \int\limits_{0}^{x}\int\limits_{0}^{y} I(x', y')G(x - x', y - y')dx'dy', \quad (1.1)$$

where the Gaussian kernel is written as

$$G(x, y) = g(x)g(y) = \frac{1}{2\pi\sigma^2}e^{-\frac{x^2+y^2}{2\sigma^2}} \quad (1.2)$$

with the width σ of the kernel. This function is very appropriate for a smoothing kernel, because firstly it is separable, and secondly its convolution with another Gaussian leads to a Gaussian again. However, the procedure makes images blurry, but this effect can be reduced by adjusting the kernel width.

Now it is useful to remark that the derivative of convolution is a well-defined mathematical operation. It satisfies an important property $(f * h)' = f * h' = f' * h$. Then the gradient representation of the smoothing image is calculated as a convolution of the original image with Gaussian derivatives of first order, one for each image dimension:

$$G_x = g(y) \cdot g'(x), \qquad G_y = g(x) \cdot g'(y), \quad (1.3)$$

which can be determined explicitly. Consequently, we obtain two different scale spaces – the horizontal gradient $I_x = I * G_x$ and the vertical gradient $I_y = I * G_y$. The extraction of different local orientation patterns is based on the following relation

$$G^{(\varphi)}(x, y) = G_x(x, y)\cos\varphi + G_y(x, y)\sin\varphi. \quad (1.4)$$

The angle φ indicates the gradient orientation fixed by an explorer. The basic idea of the reconstruction after the gradient manipulations is to find a function u whose gradient field best approximates an obtained vector field $J = I * G^{(\varphi)}$ in a least-square minimization sense. This problem leads to the unique solution of the Poisson equation $\Delta u = divJ$, where $\Delta = \frac{\partial^2}{\partial x^2} + \frac{\partial^2}{\partial y^2}$ and $divJ = \frac{\partial J_x}{\partial x} + \frac{\partial J_y}{\partial y}$ are the Laplace and divergence operators, respectively (P. Pérez et al., 2003).

Illustrative Results

To illustrate the above-mentioned approach, we consider the event recorded by the Ukrainian decameter radio telescope, UTR-2 (near Kharkiv, Ukraine) on 2 June of 2011 (Figure 1a). The major feature of solar activity in this day is a series of solar X-ray flares following each other: at 02:37 UT (GOES class C2.6, NOAA active region 11228); at 02:39 UT (GOES class C1.2, NOAA active region 11226); at 06:30 UT (GOES class C1.4, NOAA active region 11226); at 07:22 UT (GOES class C2.2, NOAA active region 11227); at

09:44 UT (GOES class C2.7, NOAA active region 11226); at 10:22 UT (GOES class C1.8, NOAA active region 11231); see in more detail http://www.solarmonitor.org/?date=20110602. This explains an inhomogeneous character of X-ray emission (see http://www.swpc.noaa.gov/ftpdir/) from the Sun. Moreover, the solar activity was also characterized by several CMEs, shock waves and different radio bursts. According to http://cor1.gsfc.nasa.gov/catalog/, the CMEs happened at 05:05 UT (narrow eruption), 06:45 UT (fast eruption) and 07:45 UT (fast and bright eruption).
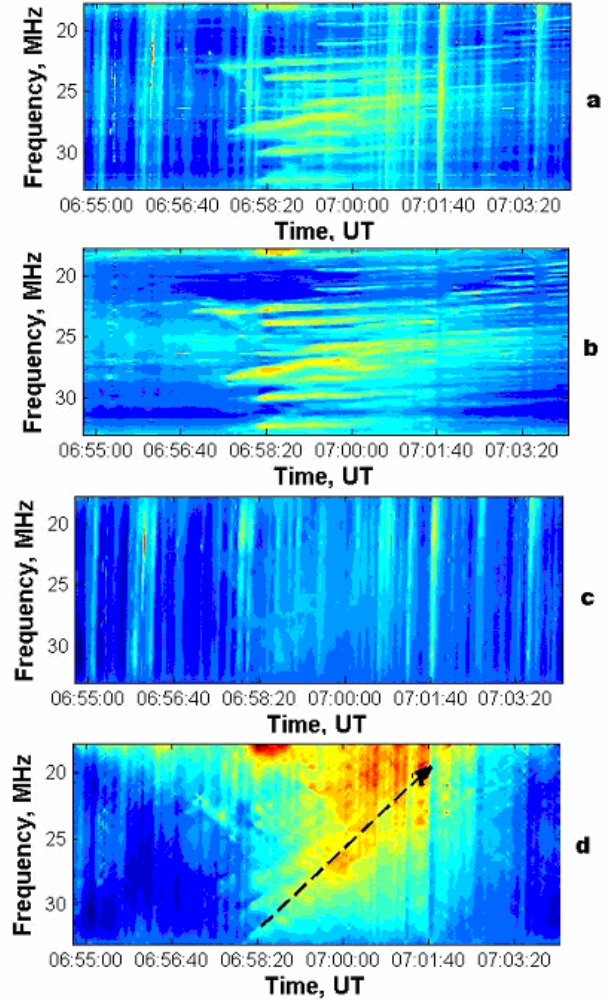

Figure 1: The dynamic spectrum of the zebra pattern, observed on June 2, 2011 by the UTR-2 radio telescope, and its gradient filtration: a) original spectrum; b) gradient filtration of zebra stripes; c) type III bursts selection; d) detection of background radio emission (see more details in the paper text).

During our observations the UTR-2 radio telescope (49°38'17" N; 36°56'29" E) was operated in the mode that includes four sections of the north-south array of the antenna. The total effective area of these four sections is equal to 50 000 m² with the beam pattern size of 1°× 15° at 25 MHz. Figure 1a shows the dynamic radio spectrum obtained by the instrument. The data were recorded by the digital DSP spectrometer (Ryabov et al., 2010) operating in the frequency range

of 16.5-33 MHz with a frequency-time resolution in ~4 kHz and ~100 ms, respectively. The unusual set of bursts was observed from 6:55 UT to 7:05 UT at the frequency range around 18-32.5 MHz. The dynamic spectrum representation consists of many horizontal strips imposed on vertical type III solar bursts. The maximum radio flux of the event reached ~10^2 s.f.u., where 1 s.f.u. = 10^{-22} W/(Hz m^2). To take off the vertical type III bursts of this dynamic spectrum, we used the gradient domain filter with the angle value $\varphi \approx 185°$ (Figure 1b). On the other hand, all the horizontal stripes may be deleted by the same filter with another angle value $\varphi \approx 90°$ (Figure 1c). This procedure gives us a chance to detect a background (Figure 1d) on which the horizontal strips hold. The background radio emission has a negative frequency drift velocity, about -0.062 MHz/s. The rate value was determined by the method of least squares to the maximum emission at each frequency. From Melnik et al. (2004) it follows that such a frequency drift rate of radio emission in the decameter range of wavelengths is representative for type II bursts due to their sources, shock waves. Assuming that the background source was a shock wave, the mean shock speed was on the order of 1057 km/s. On the dynamic spectrum the background emission strongly correlates with the frequency-time position of horizontal strips, but it does not correlate with the vertical type III bursts. Thus, the shock wave, led to the background, may be related to the quasi-periodical structure represented in Figure 1a. It should be pointed out that the background fragment is difficult to detect on the dynamic spectrum visually because it has a low intensity and is hidden by many other bursts and stripes. Although the presence of the background component can be noticed by averaging the dynamic spectrum in time, the gradient filtration procedure permits us to study the background features in more details. In particular, we have discovered its slow, negative frequency drift. Moreover, the gradient filtration helps us focus on horizontal strips and their properties. They will be interpreted in the next section.

Magnetic field strength in the solar corona

Solar radio emission is very effective in providing diagnostics for the solar plasma, especially as applied to the magnetic field in corona (see, for example, Kim et al., 2012). The coronal magnetic field strength can be measured in more than one ways: from optical observations of vector magnetic fields in the photosphere and their extrapolation into the corona (Schrijver and De Rosa, 2003); by Faraday rotation techniques (Spangler, 2005); by band splitting in coronal and interplanetary type II radio bursts (Vršnak et al., 2001); by applying the piston-shock relationship to the observed CME's standoff distance and electron density compression ratio (Kim et al., 2012); etc. One of them is the radio observation of solar bursts with zebra structure that represents several or numerous alternate bands of enhanced and reduced radiation (Aurass et al., 2003; Bárta and Karlický, 2006; LaBelle et al., 2003 and references therein). The observed frequency

spacing between stripes is explained in terms of the electron gyrofrequency $\omega_B = eB/mc$, where B is the magnetic field strength, e the electron charge, m the mass of electron, and c denotes the velocity of light (Zheleznyakov and Zlotnik, 1975). In this case the electrons with non-equilibrium distribution over velocities perpendicular to the magnetic field excite longitudinal electrostatic waves (Bernstein modes) at frequencies multiple to the electron gyrofrequency (Zlotnik, 2009).

Basic features of the event in Figure 1a can be explained on the assumption of Bernstein modes. In particular, the mechanism of Bernstein modes can provide only a few (less than 10) harmonics in the resulting spectrum. Moreover, the frequency spacing between zebra neighbor strips gives the magnetic field value, which looks quite reasonable. The zebra event originated from a highly asymmetric coronal loop (between neighboring active regions 11226 and 11227) forming a magnetic trap, when electrons were propagating along the loop, and the electron accelerator was located at those footpoints, where the magnetic flux was spatially more concentrated. All this indicates in favor of the mechanism, based on Bernstein modes, for the zebra patterns observed on 2 June of 2011.

Let us consider this radio event in more detail. Here the almost horizontal stripes are characterized by the frequency drift rate about -0.003 MHz/s. They distinctly contrast with almost vertical Type III bursts with frequency drift rates about -(2÷3) MHz/s (Figure 1). Based on frequency profiles of the dynamic spectrum, the frequency spacing between horizontal stripes is about 1.1-1.4 MHz. A slightly distorted structure of the stripes can be explained by magnetic field and plasma density inhomogeneities of the upper solar corona. If the stripes were harmonically related to the electron gyrofrequency, then the coronal magnetic field strength was ~0.43±0.05 G at the plasma frequency ~20.5 MHz that corresponds to at heights 1.8-2 solar radii (from the center of the Sun) in dependence of the electron density distribution model for the solar corona. This magnetic field strength magnitude supports the model (Gopalswamy et al., 1986) and is specified probably by features of the protracted solar minimum of solar activity. Basically the errors ± 0.05 G are determined by the distorted structure of stripes rather than the spectral accuracy ~4 kHz. Figure 2 shows processes of solar activity probably associated with the zebra pattern. The solar images were obtained by two STEREO spacecrafts. Their location relative to the Sun was optimal for observing this event.

Conclusions and Future Work

As mentioned before, the method of gradient filtration can be very useful for disassembling a complex group of different solar bursts into separate bursts, especially if they have noticeably distinguishable frequency drift rates. Here, we have tested this tool to the event on 2 June of 2011, where the zebra pattern was contaminated by many type III

bursts. Moreover, this analysis allowed us to detect one more burst located under these bursts. The interesting peculiarity of this radio event is that probably the electron stream, responsible for the given zebra burst, was initiated by the shock wave generating the "background" burst shown in Figure 1d.
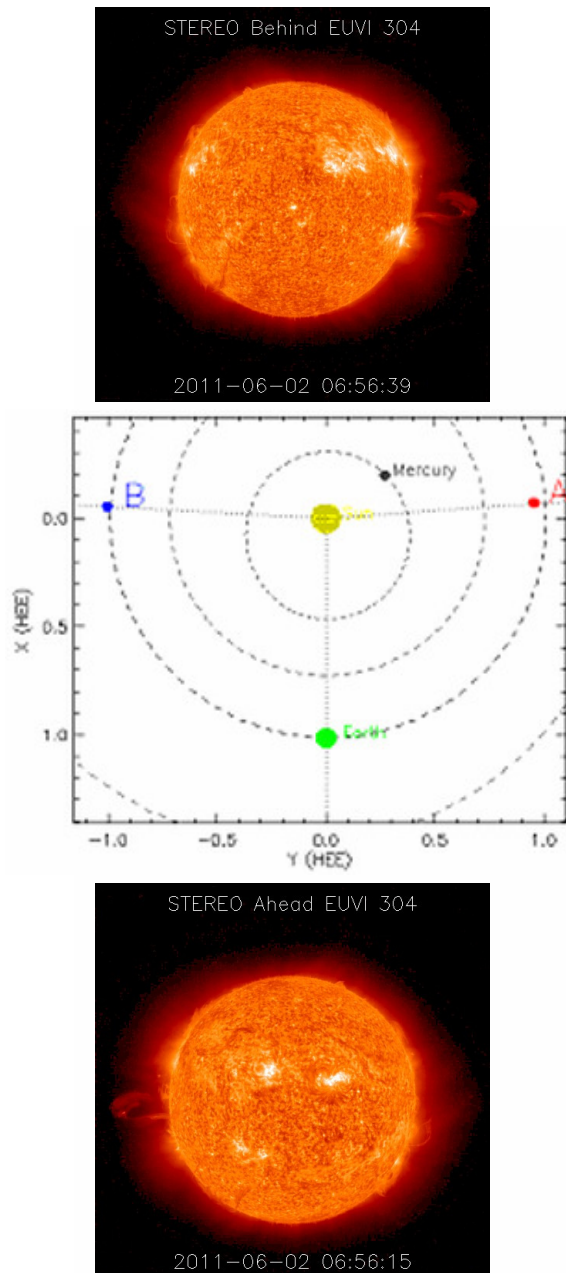

Figure 2: Ecliptic schematics (central image) on June 2, 2011 showing the positions of the planets Mercury, Venus, Earth, and Mars (and their respective orbits), along with the two STEREO spacecrafts (STEREO-A noted by A, and STEREO-B) relative to the Sun (at the centre).
Top and bottom images show the Sun at 304 Å obtained by the spacecrafts and a CME (to the Earth) probably responsible for the zebra pattern. Image courtesy of the STEREO team.

Although the detected frequency periodicity of the zebra-pattern burst gives the macroscopic magnetic field strength in upper corona, the height, where the magnetic field was characteristic, depends on a model choice for the coronal electron density distribution. This uncertainty can be overcome, for example, from the analysis of other bursts (close in time to the zebra) with features depending on the magnetic field. We plan to realize such approach in the near future. Consequently, this will allow us to establish the coronal magnetic field strength in different ways.

The obtained results confirm that the proposed approach constitutes a promising tool for investigating the evolution of solar activity and also for processing solar bursts image archives.

Acknowledgments

References

Aurass, H., Klein, K.-L., Zlotnik, E.Ya., Zaitsev, V.V.: 2003, Astron. Astrophys. 410, 1001 (doi: 10.1051/0004-6361:20031249).

Bárta, M., Karlický, M.: 2006, Astron. Astrophys. 450, 359(doi: 10.1051/0004-6361:20054386).

Fattal, R., Lischinski, D., and Werman, M.: 2002, ACM Transactions on Graphics 21(3), 249.

Gopalswamy, N., Thejappa, G., Sastry, Ch.V., and Tlamicha, A.: 1986, Bull. Astron. Inst. Czech. 37, 115.

Kim, R.-S., Gopalswamy, N., Moon, Y.-J., Cho, K.-S., Yashiro, S.: 2012, Astrophys. J. 746, 118 (doi: 10.1088/0004-637X/746/2/118).

LaBelle, J., Treumann, R.A., Yoon, P.H., Karlický, M.: 2003, Astrophys. J. 593, 1195 (doi: 10.1086/376732).

Melnik, V.N., Konovalenko, A.A., Rucker, H.O., Stanislavsky, A.A., Abranin, E.P., Lecacheux, A., Mann, G., Warmuth, A., Zaitsev, V.V., Boudjada, M.Y., Dorovskii V.V., Zaharenko, V.V., Lisachenko, and V.N., Rosolen, C.: 2004, Solar Physics, 222, 151 (doi: 10.1023/B:SOLA.0000036854.66380.a4).

Melnik, V.N., Konovalenko, A.A., Abranin, E.P., Dorovskyy, V.V., Stanislavsky A.A., Rucker, and H.O. Lecacheux, A.: 2005, Astronom. Astrophys. Trans. 24, 391 (doi: 10.1080/10556790600568854).

Pérez, P., Gangnet, M., and Blake A.: 2003, ACM Transactions on Graphics (SIGGRAPH'03) 22(3), 313.

Ryabov, V. B., Vavriv, D. M., Zarka, P., Ryabov, B. P., Kozhin, R., Vinogradov, V.V., and Denis, L.: 2010, Astron. Astrophys. 510, 16 (doi: 10.1051/0004-6361/200913335).

Schrijver, C.J., and De Rosa, M.L.: 2003, Solar Phys. 212, 165. (doi: 10.1023/A:1022908504100).

Spangler, S.R.: 2005, Space Sci. Rev. 121, 189. (doi: 10.1007/s11214-006-4719-7).

Vršnak, B., Aurass, H., Magdalenić, J., Gopalswamy, N.: 2001, Astron. Astrophys. 377, 321 (doi: 10.1051/0004-6361:20011067).

Zheleznyakov, V.V., Zlotnik, E.Ya.: 1975, Solar Phys. 43, 431 (doi: 10.1007/BF00152366).

Zlotnik, E.Ya.: 2009, Cent. Eur. Astrophys. Bull. 33, 281.